VIBRATIONAL, ELECTRONIC PROPERTIES PHARMACEUTICAL STUDY OF 4-CARBOXY-3-FLUOROPHENYLBORONIC ACID AND ABILITY TO FORM ITS DIMER BY USING DENSITY FUNCTIONAL THEORY

A.K. PANDEY[*], D.D. DUBEY[*], S.N. TIWARI[*], G. MISHRA[*], P.K. PANDEY[**], S.I. ANSARI[***], V.N. MISHRA[***#]

https://www.doi.org/10.59277/RJB.2024.4.03

[*]Department of Physics, "K.S. Saket" P.G. College, Ayodhya (UP), India
[**]Department of Physics, "G.S." College Chhapra, Bihar, India
[***]Department of Physics, "Shree Ramswaroop" Memorial Group of Professional Studies, Lucknow (UP), India, [#]e-mail: vnvictorious@gmail.com

Abstract. The motive of present article is to attract attention on conformational analysis and electronic features of 4-carboxy-3-fluorophenylboronic acid compound via computational method. To comply this, density functional theory (DFT) in combination with Becke 3-parameter Lee-Yang-Parr (B3LYP) functional was considered to identify possible conformers and hence the ground state conformation. The stability reaction of formation quantum theory of atoms in molecules (QTAIM), natural bond analysis (NBO) and thermodynamical stability of dimerization of 4-carboxy-3-fluorophenylboronic acid is computed by using DFT/6-31G(d, p) method. The Eigen value of highest occupied molecular orbital (HOMO), lowest unoccupied molecular orbital (LUMO), and related energy bandgap were computed at B3LYP. In addition to these, thermodynamic properties and nonlinear properties (NLO) are also computed. Study of NLO (nonlinear optical behavior) reveals the nonlinear properties of the title molecule. The UV-Vis spectra of title molecule were calculated by time dependent density functional theory (TDDFT/6-31G(d, p)) on optimized geometry by same level theory. The biological activity of title molecule is computed by PASS online server which predict 4000 types of biological activities, counting pharmacological effects, mechanisms of action, toxic and adverse effects, interaction with metabolic enzymes and transporters, influence on gene expression, etc. The title molecule showed good activity against antineoplastic (0.914), peptidyl transferase inhibitor (0.969), aminoacylase inhibitor (0.960), sugar-phosphatase inhibitor (0.913), ribulose-phosphate 3-epimerase inhibitor (0.896), antiviral (0.862), TP53 expression enhancer (0.860). To determine anti-inflammatory potential, we have performed docking of title molecule with drosophila, which is a muscleblind like splicing regulator 1 (MBNL1) protein, by using Swiss dock online server.

Key words: DFT, HOMO, LUMO, NLO, 4-carboxy-3-fluorophenylboronic acid.

INTRODUCTION

The boronic acid moiety has essentially been a part of various biologically important compounds. It does not exist naturally; still it has appeared since 1860 in

Received: February 2024;
in final form November 2024.

ROMANIAN J. BIOPHYS., Vol. 34, No. 4, P. 213–236, BUCHAREST, 2024

the literature [18]. Stability, exclusiveness and handy reactivity shown by boronic acids, made it a key precursor in numerous areas, including acid catalysis, formation of C–C bond, carbohydrate analysis, asymmetric synthesis, molecular sensing, metal-catalysis, and as an enzyme inhibitor, therapeutic agents, and a novel material [13, 46, 57]. From last decade boron pay lot of attention in drug designing area due to its useful biological activities [15]. Edward Frankland was firstly synthesized boronic acids in 1860 [18, 19]. The boronic acids can be utilized as building blocks and synthetic by product [23]. The versatile reactivity, stability, and low toxicity of boronic acids play important role in by product in synthetic chemistry [8, 24]. In drug designing, boronic acid is further decomposed into boric acid, the finally removed by the human body [49]. Boronic acids have unique physicochemical and electronic characteristics [58]. One of important use of boronic acid is in treatment of various types of cancer cells, like breast cancer [54]. In early period of 19th century, boric acid (B(OH)3) was used as minor antiseptic. Now a day, boron-based drug show much therapeutic potential attention [2, 6]. In 2003, boronic acid-containing drugs [22] was approved by the U.S. Food and Drug Administration (FDA). The crisaborole [16] and vaborbactam [35] are utilized in treatment of atopic dermatitis and bacterial infections, respectively. Other boron containing drugs are also under clinical trial [3]. The trigonal [52], tetragonal covalent [23] with nucleus loving residue, *e.g*. serine, lysine, tyrosine, are present in target proteins with boronic acids. The two hydroxyl groups with four lone pairs with two hydrogen bond presents on boronic acids which provides more opportunities to bind with amino acid residues. The interacting hydrogen bonds are small, however high interacting energy of boronic acid with target protein increase the binding affinity of the inhibitor with boronic acid [49, 55]. The boronic acid shows extra interaction property to interact with metal ions in enzymes [11]. The diversity of boronic acid derivatives of different organically significant materials has been produced to aim at a possible two split attack on cancer as anti-metabolites [11, 54]. The moiety of boronic acid has also been fused with amino acids and nucleosides as anti-viral agents, anti-tumor [1]. Many authors have been reported molecular structure as well characteristics of phenylboronic acid, and also for its by-products for years [45, 56]. The crystal structure of phenylboronic acid has been studied by Rettig and Trotter [45]. Literature investigation divulges no comprehensive theoretical or experimental DFT study of 4-carboxy-3-fluorophenylboronic acid (4C3FPB) so far. In ongoing communication, we mainly focused on the detailed conformal analysis using DFT/B3LYP calculations for 4C3FPB. Furthermore, the entropy, heat capacity, and enthalpy were examined at room temperature and their variations with the temperature have been plotted. In addition to these, energy of HOMO and LUMO, and NLO (first order static hyperpolarizability β and related other properties like Δα and ‹α› features of 4C3FPB were also calculated. The biological activities of 4C3FPB on optimized geometry, by using same level theory, are also calculated, however docking of 4C3FPB has been done by appropriate protein. The binding

strength are calculated by using binding affinity full fitness score. The present communication explores various possibilities of 4C3FPB appropriate binding with suitable protein. We hope our research opens new pathway in therapeutic industry.

COMPUTATIONAL DETAILS

The initial geometry C3FPB molecule is designed, and initial geometry is optimized by using combination of DFT [32] and hybrid B3LYP functional [7, 31, 50], as well as basis set 6-311++G(d, p). The various properties of 4C3FPB are obtained with computational techniques which offers a decent explanation on moderate-sized molecules. In this work, Gaussian 09 program package [20] was involved to perform all types of calculations and outcomes were analyzed with molecular visualization program Gauss view 5.0 [19]. The stability in geometry of title molecule was resolute using PES (potential energy scan) via changing torsional angles C4-B10-O13-H14 and C4-B10-O11-H12 at B3LYP/6-31G(d) level of theory. The stability of dimer of title molecule is also studied by using thermodynamical parameters of reaction and QTAIM analysis of most stable dimer. The variation in electronic properties of dimer and monomer are also studied by using several chemical reactivity parameters based on energy of HOMO, LUMO molecular orbital. The UV-Vis spectrum for optical absorption of title molecule is calculated by using TDDFT (time dependent DFT) on optimize geometry of title molecule. The vibrational analysis of the title molecule is compared with its dimer which also has been done on its optimized geometry by using the same level theory. The assignment of vibrations is calculated by using Gauss View 6.0 program. The overestimation in calculated frequencies has been observed due to vibrational analysis done on single molecule with harmonic approximation. To compare with observed vibrational spectra scaling of calculated frequencies is required. The biological activity of title molecule is calculated by using PASS online server. The initial input of the optimized geometry of title molecule was uploaded in SIMILI code. The ALOGPS 2.1 program based on electro topological indices [28, 54, 55] are used to calculate transport properties like log *P* and log *S* of title molecule. The prediction of target protein for docking with title molecule has been done by using Swiss Dock online server [59]. The docking of title molecule with predicted protein MBNL1 was also performed by Swiss Dock online server. The strength of docking of title molecule with target drug are determined by full fitness score (*FF*) binding affinity, length of H-bond, etc.

ESTIMATION OF VARIOUS NONLINEAR OPTICAL PROPERTIES (NLO)

The finite field approach was considered to calculate various nonlinear optical properties, *e.g.* dipole moment (μ), mean polarizability ‹α›, anisotropy of the polarizability (Δα), and total first static hyperpolarizability β [30, 47]. This method proposes orthodox tactic for computing hyperpolarizability [12]. These properties

play an important role to elucidate a reaction of molecular system in an applied electric field. In terms of variables *x*, *y* and *z*, the dipole moment μ, mean polarizability ‹α›, the polarizability (anisotropy) Δα, and first order static hyperpolarizability β are computed by using following equations:

$$\mu = \sqrt{\mu_x^2 + \mu_y^2 + \mu_z^2} \quad (1)$$

$$\langle\alpha\rangle = \frac{\alpha_{xx}+\alpha_{yy}+\alpha_{zz}}{3} \quad (2)$$

$$\beta_x = \beta_{xxx} + \beta_{xyy} + \beta_{xzz} \quad (3)$$

$$\beta_y = \beta_{yyy} + \beta_{yzz} + \beta_{yxx} \quad (4)$$

$$\beta_z = \beta_{zzz} + \beta_{zxx} + \beta_{zyy} \quad (5)$$

in this system: for polarizability α, 1 a.u. = 0.1482×10^{-24} e.s.u. (electrostatic unit), and for hyperpolarisability β, 1 a.u. = 8.6393×10^{-33} e.s.u.

RESULTS AND DISCUSSION

POTENTIAL ENERGY SCAN AND GEOMETRY OPTIMISATION

Potential energy scan

The 4-carboxy-3-fluorophenyl boronic acid has three substituents group $B(OH)_2$ group (with two –OH group joined with boron), –COOH group at ortho position and at meta position F (fluorine) atom. The three substituents (F, COOH and $B(OH)_2$) on the ring are selected such that four stable isomers of the title molecule (Fig. 1) are possible. The four-probable geometry of 4-carboxy-3-fluorophenylboronic acid are analyzed by position of hydrogen (–OH group) whether they are pointed toward or away from the ring. To explain conformational analysis of 4-carboxy-3-fluorophenylboronic acid, the PES scan is performed in between phenyl ring and B(OH)2 group system. To envisage the stable ground state conformer of 4-carboxy-3-fluorophenylboronic acid (4-C3FPB), a 3-D potential energy surface (3D-PES) scan was executed by changing torsional angles C4-B10-O13-H14 and C4-B10-O11-H12 in the steps of 10º from –180º to +180º at DFT/B3LYP/6-31G(d) method. Throughout the scan, entire geometrical structures were concurrently comfortable, except two designated dihedral angles. To find conformational flexibility inside the title molecule, dihedral angles C4-B10-O13-H14 and C4-B10-O11-H12, which are the relevant torsional angles related to torsional profiles of the PES scan, are plotted in Fig. 1. The conformers which are stable – trans-trans (minima points A), trans-cis (minima points B), cis-trans (minima point C), and cis-cis (minima point D) are reflected on PES (Fig. 1).

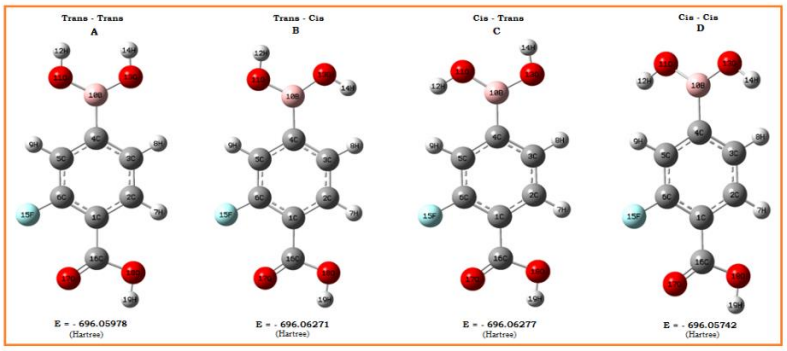

Fig. 1. Four stable conformers of 4C3FPB along with their energies.

The position of the OH group in the title molecule is represented by trans-conformer (headed away from the ring) and by cis-conformer (headed toward the ring). Energy values attained from outcome of the PES scan discloses that the conformers at minima point B and point C in trans-cis and cis-trans alignment are much stable in comparison with conformer at minima A and minima D in trans-trans and cis-cis alignment, according to –OH position. The energy deviation among two lower conformers (trans-cis and cis-trans) is 0.00006 Hartree only at DFT/B3LYP/6-31G(d). The lesser energy conformer is cis-trans conformer; so further 2D PES scan has executed on cis-trans conformer by varying dihedral angle C3-C4-B10-O13 from –180º to +180º in steps of 10º, to check the orientation of complete boronic acid group along phenyl ring.

Molecular geometry

The lowest energy structure of 4C3FPB obtained after conformational analysis was once again optimized at higher basis set 6-311++G(d, p) with same level of theory. Figure 2 depicts the optimized geometry of 4C3FPB with labelling scheme of atoms which contains the optimized geometric parameters like lengths, angles and torsional angles related to bonds. The crystal structure of molecules under investigation are unavailable, thus optimized structure of 4C3FPB was compared with some other molecular systems having identical groups, like phenylboronic acid and 3-fluorophenylboronic acid [45, 56]. In 3-flurophenylboronic acid [56], bond lengths of C–C (ring) were detected between 1.365–1.406 Å, and from 1.378 to 1.404 Å for the phenylboronic acid [45]. In the present study, the bond lengths C4-C5, C3-C4, C1-C2 varies between 1.399–1.406 Å, and are longer than bond lengths C2-C3 (1.386 Å), C5-C6 (1.387 Å). The reason for this is partial double bond character. Literature [45] shows that the O–B bond length for phenylboronic acid is 1.362 Å and 1.378 Å. Similarly, it is 1.343 Å and 1.366 Å in context of 3-fluorophenylboronic acid [56]. These distances were computed at 1.364 Å (O13-B10) and 1.371Å (O11-B10) that presents a fair association with architecturally like compounds.

Bond length C–B are observed at 1.568 Å for phenylboronic acid [45] and 1.562 Å for 3-fluorophenylboronic acid. In the current study, bond length C–B is calculated as 1.573 Å for 4C3FPB. Theoretical calculation shows that C–H bond lengths for 4C3FPB are almost equal to C–H bonds for 3FPBA [56].

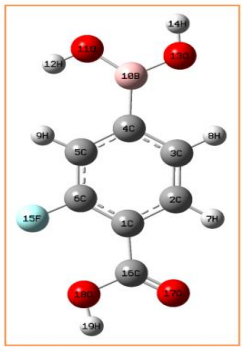

Fig. 2. Optimized geometric structure of 4C3FPB.

The bond length C–X, where X may be F, Cl, Br, etc., demonstrates an extraordinary escalation when replaced X at the position of hydrogen atom. In present work, the C–F bond length is computed as 1.346 Å at B3LYP/6-311G++(d, p), showing good coherence with similar molecule [56]. A noteworthy deviation in bond angles C–B–O and also in O–B–O from the predicted value 120 º angle is detected with a reason of acquiring sp2 hybridized state by boron. Resonance interaction among vacant p orbital of boron and oxygen lone pairs may perhaps restrict H10 and H11 (both) of boronic group to remain in plane of O–B–O. All computed geometric parameters are in a sound coherence with consistent experimental data. The C–C–C bond angles of six-member ring were generally perceived in the range 117.60–123.90 in degree for 3-fluorophenylboronic acid [56], and are in better association (excluding some) with the standard angle in degree (120.00) for the ring. Moreover, C1–C6–C5, C3–C4–C5 and C2–C1–C6 bond angles of title compound diverged more from standard value; it is due to the attached heavy atom/group like fluorine atom, carboxylic and boronic group. Anyone can effortlessly observe from above data that calculations of the angles in 4C3FPB are consistent and proximate to associated experimental data of structurally analogous compounds [45, 56].

DIMER FORMATION OF 4C3FPB

Dimer geometry

To study dimer of title molecule we have designed four possible conformer (Fig. 3) by placing first unit with respect to second unit and design geometry of dimer optimized by using DFT/6-31++G(d, p) method. In first conformer oxygen (–C=O) of

first unit with –HO of second unit and vice versa. After geometry optimization by using DFT/6-31++G(d, p) method, the optimized geometry having an energy of –1180.347 a.u. However, in second conformer, both units are placed perpendicular to each other and after optimization by same level theory the optimized energy is –1121.254 a.u. The third conformer is similar with the second, except second unit rotate 180º. After geometry optimization, calculated energy of third conformer is –1089.687 a.u. In forth conformer (helps to understand the stability based on energy of isomers) both units are placed parallel in such a way that F atom of first unit interact with hydrogen of the second unit and vice versa. However, optimized energy of conf-04 (conformer-4) is slightly higher than conf-01. The minimum energy corresponds to conf-01; that means that the most probable geometry of conformer of dimer of title molecule is first one.

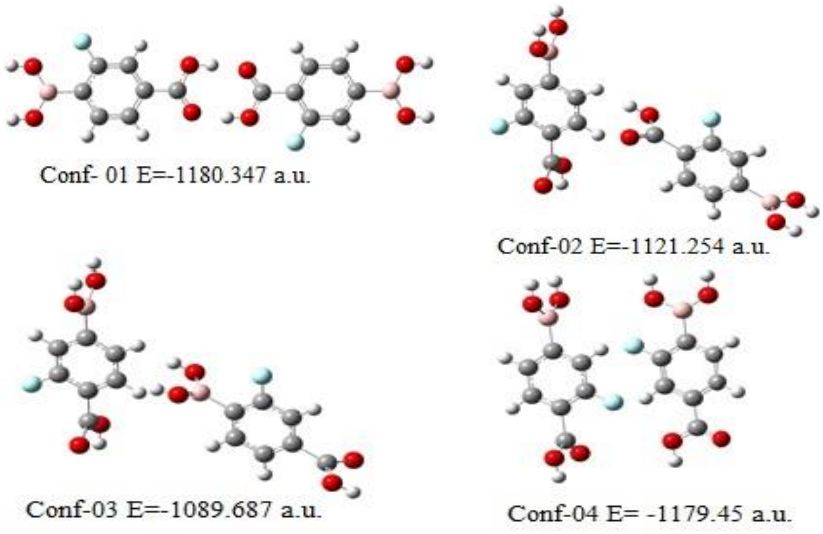

Fig. 3. Various conformer of dimer along with optimized energy.

QTAIM analysis

At bond critical point (BCP), inter and intra molecular interaction in any chemical system is calculated by using quantum theory in atom (QATIM) analysis with help of some topological parameters. In nonbonding interaction electron density (ρ_{BCP}) and Laplacian ($\nabla^2\rho_{BCP}$) should lies in between 0.002–0.040 a.u., and 0.024–0.139 a.u. respectively [31]. Based on above criteria, two nonbonding interaction appears O37-H14, H38-O19 in dimer formation (Fig. 4). Several topological parameters like electron density ρ_{BCP}, kinetic energy $G(r)$, potetial energy $V(r)$ and total energy $H(r)$ (r represents the position vector of the molecule) at BCP in dimer are calculated and listed in Table 1. The nature of nonbonding interaction is

determined by Laplacian $\nabla^2\rho(r)$. The $\nabla^2\rho(r) \geq 0$ and $\rho(r)$ are of order of 10^{-2} for both interactions which indicate that both interactions are closed shell H-bonding [5]. The value of $\nabla\rho(r)$ very close to limit of nonbonding interactions however $\rho(r)$ varies from 0.057–0.058 a.u. The value of total energy is the sum of kinetic and potential energy; that means $H(r) = V(r) + G(r)$ at BCP. The value of $H(r)$ is an important factor to know about nature of chemical bonds. In this calculation, $V(r) > G(r)$; that means $H(r) < 0$, and shows in both interactions sharing of electrons dominates means less ionic nature. One important parameter magnitude of ratio of potential energy to kinetic energy I (a critical concept in determining the balance of forces that keep the molecule in stable) is found to be greater than one (Table 1); this again establish its covalent nature [50]. The value of I greater than one indicates that for both interactions (nature of nonbonding interactions and nature of chemical bond) calculated and found $\nabla^2\rho_{BCP} > 0$ and $H(r) < 0$ again shows their covalent nature. The strength of interaction energy is computed by using following equation [14].

$$E_{int} = \frac{1}{2} \left| V_{BCP} \right| \tag{6}$$

where E_{int} is the energy of interaction of molecules of dimer and V_{BCP} is the potential energy at bond critical point. The value of E_{int} is calculated in kcal/mol, which is obtained by conversion of 1 a.u. energy into kcal/mol by a conversion multiplier of 627.51.

Table 1

Various topological parameter of dimer at bond critical points (BCP)

Bond	ρ_{BCP} (a.u.)	$\nabla^2\rho_{BCP}$ (a.u.)	G_{BCP} (a.u.)	V_{BCP} (a.u.)	$\left\| \frac{V(r)}{G(r)} \right\|$ (or I)	H_{BCP} (a.u.)	E_{int} (kcal/mol)
O37-H14	0.057	0.131	0.0526	–0.0726	1.380	–0.020	22.78
H38-O19	0.058	0.131	0.0525	–0.0726	1.380	–0.021	22.78

By calculation, we have found that the value of interaction energy of dimer for both molecules are > 12 kcal/mol, which shows that both interactions are fall in weak category.

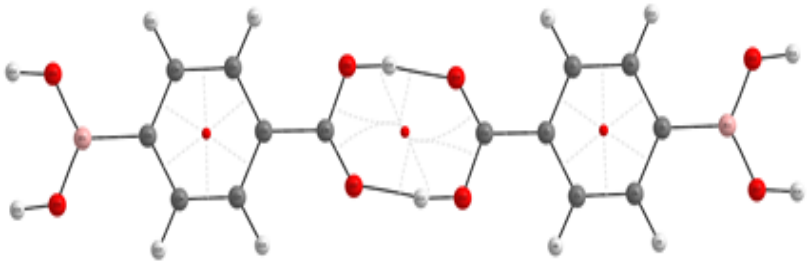

Fig. 4. QTAIM picture of dimer: The small red dots represent the ring critical points (RCP), and other point are atoms (red – O, black – C, brownish white – H, pink – B).

Nonbonding orbitals analysis (NBO) of dimer

The nonbonding orbitals analysis (NBO) of any system is an important tool to determine nonbonding interaction in molecule. The NBOs provides an effective basis for examining charge transfer or conjugative interaction in any chemical system [9]. The value of second order interaction energy E(2) provides intensity among electron donors and electron acceptors, The charge transfer from one unit (1) to unit (2) due to n1(O37) $\rightarrow$ ⌠σ*(O13–H14)], n3(O19)$\rightarrow$ ⌠σ*(H38–O32]) stabilized dimer of title molecule up to 61.88 kcal/mol and 45.66kcal/mol respectively proves interaction O37–H14 and H38–O19 (σ* shows antibonding charge density).

Thermodynamical stability of 4C3FPB dimer formation reaction

Let us check stability of dimer formation of title molecule by using DFT/6-31G(d, p) method.

Adsorption energy for the reaction is given by the following equation:

$$E_{\mathrm{ad}} = E(\text{dimer}) - 2\,E(\text{4-carboxy-3-fluorophenylboronic}) \qquad (7)$$

The computed electronic energy for reaction ($E_{\mathrm{ad}} < 0$) means that dimerization of title molecule proceeds in forward direction. The K_{eq}, thermodynamical equilibrium constant for dimerization is calculated by $\exp^{-\frac{\Delta G}{\mathrm{R}T}}$. The intended equilibrium constant for dimerization indicate that dimerization of title molecule is highly favored at T = 300 K.

The computed thermodynamical parameters for dimerization reaction at T = 330 K are listed in Table 2. The computed Gibbs free energy (ΔG), enthalpy (ΔH), and entropy (ΔS) for dimerization of title molecule are negative. It indicates that dimerization of 4-carboxy-3-fluorophenylboronic is exothermic and spontaneous at T = 300 K.

Table 2

Various calculated thermodynamical parameters of dimer formation reaction at T = 300K

SN	Parameter	Title molecule	Dimer	Reaction
1	Electronic energy (a.u.)	–590.001827	–1180.04582	–1.14737
2	Gibbs free energy (a.u.)	–590.038136	–1180.0996	–0.63477
3	Enthalpy (a.u.)	–589.990874	–1180.02455	–1.16467
4	Entropy (kcal/mol)	99.471	159.995	29.35
5	*K*eq	–	–	4889.5

ELECTRONIC PROPERTIES

The highest occupied molecular orbitals (HOMO) and lowest unoccupied molecular orbitals (LUMO) are useful molecular orbitals to determine nature of

electronic properties of any chemical system. The HOMO and LUMO are known as frontier molecular orbitals. The energy required to transfer electron from HOMO to LUMO are known as energy band gap of any system. Moreover, LUMO and HOMO regulates the approach of molecular interaction with external species. Key descriptors of reactivity – 'hardness and softness' are generally associated with the HOMO–LUMO energy gap. A hard molecule exhibits vast LUMO–HOMO gap, and is anticipated to be less reactive in terms of chemical reactivity; that means that hardness is directly linked with chemical stability. A less energy gap of LUMO–HOMO, on other way, designates a soft molecule [17]. Several electronic reactivity descriptors of monomer and dimer of 4-carboxy-3-fluorophenylboronicare calculated and listed in Table 4 by using DFT/6-31G(d, p) method.

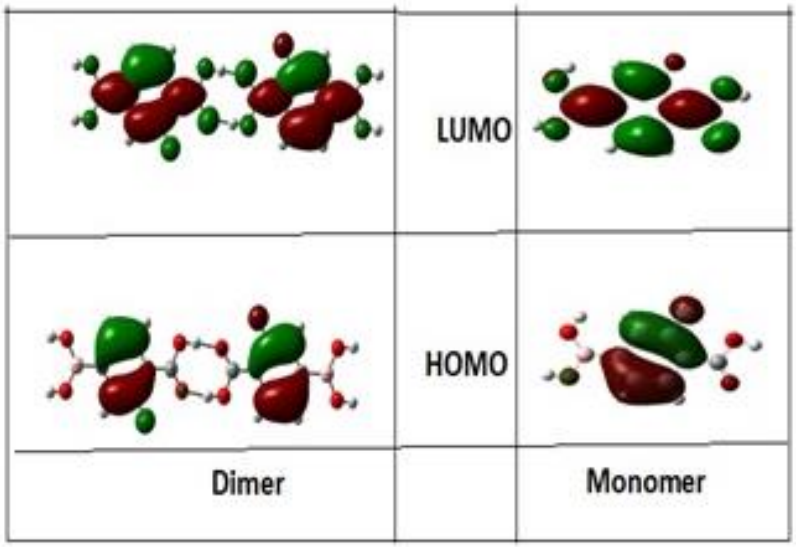

Fig. 5. HOMO LUMO plot of monomer and dimer of 4C3FPB.

The three-dimensional plots of frontier molecular orbitals compositions are revealed in Fig. 5 predict that HOMO is homogeneously distributed over the whole molecule except boronic acid and carboxylic group; however, in dimer HOMO is distributed over whole molecule except carboxylic group of both interacting units. The LUMO spreads over whole molecule in both monomer and dimer. The HOMO energy monomer lies lower energy than dimer, however, LUMO shifted higher energy in dimer as compared with monomer coequally calculated band gap in dimer (4.59 eV) is less than band gap of monomer (6.71 eV). The enhance reactivity in dimer as compared with monomer is due to polarity arise by nonbonding interaction of both units. The negative eigen value of HOMO and LUMO are known as ionization potential and electronegativity. The chemical potential [42] is equal to

negative of absolute electronegativity (χ); however absolute electronegativity (χ) is negative average of ionization potential and electronegativity. Maximum hardness [44] theorem states that highest possible energy gap in between HOMO and LUMO energy means the highest value of g (absolute hardness) and correlates with the stability [38]. Chemical hardness measures the difficultness of reaction of the title molecule with molecules of other chemicals. Similarly chemical softness measures the easiness of reaction of title molecule with molecules of other chemicals. According to quantum theory, mixing of ground state wave function with excited state wave function gives optical polarizability. The exciting energy from ground state to excited state is inversely proportional to mixing coefficient. The chemical hardness any system is half of energy gap in between HOMO and LUMO energies. One important point noticed that amount of a chemical system's acceptance to deviations in electron distribution is defined by global chemical hardness and is associated to its stability as well as chemical reactivity. The global softness is reverse of global hardness and vice versa. The calculated global hardness of monomer is greater than that of dimer, and calculated global softness of monomer is smaller than that of dimer of the title molecule. The computed values of global softness and global hardness of monomer and dimer of title molecule establish their chemical stability.

Table 3

Calculated electronic parameters in of monomer and dimers of title molecule

Species	HOMO (eV)	LUMO (eV)	ΔE_{gap} (eV)	χ (eV)	μ (eV)	η (eV)	s $(eV)^{-1}$	ω (eV)
Monomer	–8.96	–2.25	6.71	5.61	–5.61	3.35	0.149	4.70
Dimer	–6.58	–1.99	4.59	4.29	–4.29	2.28	0.218	4.02

χ – absolute electronegativity, μ – chemical potential, η – chemical hardness, s – chemical softness, ω – electrophilicity.

UV-VIS SPECTRA OF 4C3FPB

The TDDFT method is utilized to calculate optical spectra (UV-Vis) of title molecule on optimized geometry by using DFT/6-31G(d, p) method. The TDDFT calculation are done up to sixteen excited energy state. In UV spectra (Fig. 6), six absorption peak appears. The electronic transition energy and transition molecular orbitals along with % contribution of orbital and maximum wavelength and oscillatory strength are listed in Table 4. The most intense peak calculated at 168 nm due to S0→S4 with oscillatory strength (f = 1.098 cm^{-1}) having electronic transition energy of 2.626 eV. The transition corresponds to H-1→L contribute 81 %. Two less intense peak appears at 161 nm with f = 0.339 cm^{-1} and 214 nm with f = 0.339 cm^{-1} due to transition in between S0→S5/S2 with a transition energy of 2.636 eV and 3.716 eV, respectively.

Table 4

Calculated electronic transitions: state transition energy *E*, oscillatory strength, *i.e*. *f*, and λ_{max} of title molecule

Excited state	*E* (eV)	*f* (cm^{-1})	Calculated λ_{max} (nm)	Transition orbital's
S0→S1	2.634	0.135	216	H-1→L(41 %), H→L (85 %)
S0→S2	2.636	0.339	214	H-1→L (81 %)
S0→S4	3.281	1.098	168	H-1→L (13 %), H→L+1 (84
S0→S5	3.716	0.614	161	H-1→L+1 (88 %)
S0→S8	3.718	0.148	139	H-3→L(55 %), H-3→L+2 (11 %), H-1→L+2 (19 %)
S0→S35	3.852	0.129	120	H-4→LUMO (69 %), H-4L+2 (–20 %)

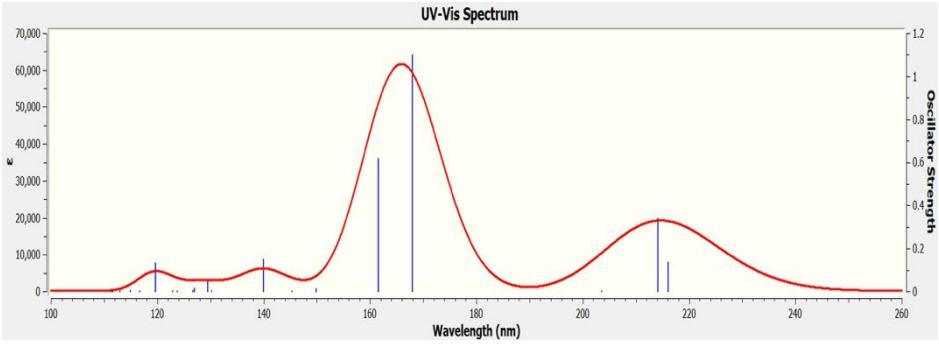

Fig. 6. UV spectrum of title molecule (wave number and oscillatory strength in vertical axis are in cm^{-1}).

NLO analysis

Nonlinear optical (NLO) effects ascend from the interactions of electromagnetic fields in several media to reform different fields with amended frequency, amplitude, and phase, or other propagation features from the applied field [53]. NLO is a state-of-the-art of present-day research considering its vital use in explicates the pivotal roles of optical switching, logic, memory and optical modulation and frequency shifting, for evolving technologies in the areas like broadcastings, and signal processing [4, 22]. NLO methods are also well-thought-out as unique structure-sensitive methods to understand the molecular structures and assemblies. Meanwhile the prospective of organic materials for NLO devices have been proven. The density functional theory provides important information in between electronic structure and NLO response. To explore the NLO features of a molecular system, archetypal molecule like urea is used for comparative task frequently as an edge value. Some important nonlinear optical parameters of title

molecule are calculated and listed in Table 5. The intended values of μ, ‹α› and βtotal for the titled molecule are 2.2711 D, 16.3361 × 10^{-24} e.s.u. and 1.1984 × 10^{-30} e.s.u. by same level theory. The 4C3FPB comprises huge β_{total} value higher than urea (0.1947×10^{-30} e.s.u.), which specifies, title compound can be a decent aspirant for NLO material. Theoretical calculations are more valuable to resolve of specific components of β tensor there after founding the real values of β. Supremacy of specific components demonstrates significant delocalization of electronic charge in respective directions. The extreme values of hyperpolarizability in β_{xxx} direction are perceived that refers that electron cloud is delocalized in that side more.

Table 5

The computed values of μ, α, β (a.u.) for 4-carboxy-3fluorophenylboronic acid

Electronic properties	Parameters	B3LYP/6-311++G(d, p)
Dipole moment (debye)	μ_x	–1.7914
	μ_y	1.376
	μ_z	0.2345
	μ	2.2711
Polarizability (a.u.)	α_{xx}	157.133
	α_{xy}	–3.054
	α_{yy}	114.321
	α_{xz}	0.136
	α_{yz}	–0.173
	α_{zz}	59.238
	‹α›	16.3361 × 10^{-24} e.s.u
	Δα	81.9984 × 10^{-24} e.s.u.
First order static hyper polarizability (a.u.)	β_{xxx}	179.012
	β_{xxy}	–39.933
	β_{xyy}	–47.996
	β_{yyy}	–47.802
	β_{xxz}	6.939
	β_{xyz}	5.067
	β_{yyz}	4.318
	β_{xzz}	–31.064
	β_{yzz}	–13.436
	β_{zzz}	5.427
	β_{total}	143.1922 a.u.
	β_{total}	1.1984 × 10^{-30} e.s.u.

VIBRATIONAL ANALYSIS

Title molecule has 19 atoms, so it contains 3N-5 (=52) modes of vibration. In 52 modes of vibration N–1 (18) are stretching modes and rest are bending modes. The whole vibrational spectra of title molecule divided in two parts above 1000 cm^{-1}

are called functional group region, and below 1000 cm^{-1} are called fingerprint region. The calculated frequencies are containing some higher values as compared with observed values. Due to ignorance of anharmonicity of electron-electron correlation, molecular interaction in calculated result is omitted; however, these effects are observed in experimental result. To compare calculated frequencies with observed ones, we have scaled calculated frequencies by 0.96 [37]. The scaled frequencies, IR intensity and modes of vibration for monomer and dimer are listed in Table 6 and Table 7. Some selected scaled modes of vibrations for monomer and dimer are discussed below.

–C–H modes of vibration

The –CH group present on benzene ring so –CH stretching modes appear in vibrational analysis. In general C–H stretching vibrations appear in the region 3000–3100 cm^{-1}, which is the typical region for identification of the C–H stretching vibration [37]. In the present study, C–H stretching vibrations are calculated at 3415cm^{-1} to 3382 cm^{-1} for monomer with significant intensity; however, corresponding stretching modes appears at 3384 cm^{-1} to 3415 cm^{-1} with higher intensity in dimer. In the middle region of the spectra, some bending modes appear incorporate with –C=C stretching modes of vibration. In plane –CH bending modes start appearing from 1792 cm^{-1} in monomer, however corresponding bending modes start appearing from some lower frequency 1328 cm^{-1} in dimer. In dimer, –CH in-plane bending modes appear at 809 cm^{-1} with significant intensity. In lower the frequency region of the spectra, –CH out of plane bending modes appear at 816 cm^{-1} and 702 cm^{-1} in monomer and dimer, respectively.

–O–H modes of vibration

The –OH group is present in title molecule, so O–H stretching modes of vibration appears in calculations. In general, –OH stretching modes of vibration appears in between 3700–3800 cm^{-1} [37]. In our calculation –OH stretching modes of vibration appears at 3889 cm^{-1} in monomer, however corresponding stretching modes appears in dimer at 3944 cm^{-1}. Noted that polarization appears in dimer due to nonbonding interaction in dimer, in which –OH group involved so corresponding –OH stretching modes appears at lower frequency region with significant intensity. In lower frequency region, some mixing band along with –OH bending modes appears at 407 cm^{-1} and 1066 cm^{-1} in monomer and dimer respectively.

–C=O modes of vibration

The carbonyl absorption modes of stretching vibration appears due to vibration of both C and O atoms with equal amplitude, hence shown significant intensity. In dimer, –C=O group involves in nonbonding interaction, so in dimer –C=O stretching

modes of vibration appears at lower frequency region with significantly high intensity. In monomer, the –C=O stretching modes appears at 1941 cm^{-1}, however corresponding modes appear at 1838 cm^{-1} in dimer.

–C=C modes of vibrations

The substitution of heavy substituent, the band tend to shift somewhat lower wavenumber and greater the number of substituents on the ring broader the absorption region [37]. The semi-circle stretching, known as C–C aromatic stretch, in monomer are lying in between 1307 cm^{-1} to 1725 cm^{-1}, however corresponding aromatic stretching modes in dimer lies in between 1304 cm^{-1} to 1792 cm^{-1}. The C–C stretching modes may be according with opposite quadrant of ring stretching, however superseding quadrants contract which is followed by literature [37]. At lower frequency region, CC in plane bending modes appear in both monomer and dimer with significant intensity. At lower frequency region some out of plane CCC bending modes which is described in such a way that every carbon of sextant going up out of the plane while intervening carbon of sextant going down of plane are appearing in both monomer and dimers are also supported by literature.

Boron including modes of vibration $–B(OH)_2$ group attach benzene ring so –BC, –BO are present on title molecule. The –BO stretching modes of vibration appears at some lower frequency region due to greater reduced mass. The calculated –BO stretching modes of vibration appears at 1497 cm^{-1} with significant intensity in monomer however corresponding frequencies calculated at 1496 cm^{-1} in dimer. The other –OBO bending modes appear at 62.27 cm^{-1} in monomer, however corresponding modes appear at 62.41 cm^{-1} in dimer. The other modes of vibration along with mixing of other modes vibration for dimers are listed in Table 6.

Table 6

Calculated frequencies, scaled frequencies, IR intensity and vibrational assignment of dimer of 4C3FPB

S.N.	Calculated wavenumber (cm^{-1})	Scaled wavenumber (cm^{-1})	IR intensity (a.u.)	Assignment
1	3948	3790	22.2124	υ(υ(O17-H18, O15-H16)+υ(O35-H36, O33-H34))
2	3948	3790	215	$υ_{as}$(υ(O17-H18, O15-H16)+υ(O35-H36, O33-H34))
3	3944	3786	20.2685	$υ_{as}$(O35-H36, O33-H34)
4	3944	3786	18.5783	$υ_{as}$(O17-H18, O15-H16)
5	3292	3160	5802.13	$υ_{as}$(O13-H14, O32-H38)

6	1859	1785	1105.499	β_{in}(H14-O13-C12, H38-O32-C30)+υ(O19-C12, O37-C30)
7	1597	1533	426.7321	β_{in}(H14-O13-C12, H38-O32-C30)
8	1554	1492	224.3089	β_{in}((C12-C2, H8-C3, C4-H9, C1-H7, C6-H10, C5-B11)R1+(C22-C30, C21-H27, H26-C20, C24-H29, C23-H28, C25-B31)R2+(H18-O17-B11, H34-O33-B31) υ_{as}(O15-B11, O35-B31)
9	1497	1437	653.41	β_{in}(H8-C3, C4-H9, C1-H7, C6-H10)R1+(H27-C21, C20-H26, C24-H29, C23-H28)R2)+υ_{as}((C2-C3, C6-C5), (C1-C2, C5-C4))R+υ_{as}(C2-C12, C5-B11)
10	1495	1435	804.7365	β_{in}(H8-C3, C4-H9, C1-H7, C6-H10)R1+(H27-C21, C20-H26, C24-H29, C23-H28)R2, H16-O15-B11, H36-O35-B31, H14-O13, H38-O32)+υ_{as}((C5-B11-O17, C25-B31-O33)
11	1124	1079	535.5659	β_{out}(O13-H14, O32-H38)
12	1033	992	386.3101	β_{in}(H16-O15-B11-O17-H18, H36-O35-B31-O33-H34)
13	1028	987	44.3736	β_{out}((H)R1, (H)R2)
14	956	918	684.3377	β_{in}(H18-O17, H16-O15, H36-O35, H34-O33)
15	809	777	127.9913	β_{out}((H8, H9)R1, (H29, H26)R2, C12-O13-H14, C30-O32-H38)
16	702	674	376.9706	β_{out}((H7, H8)R1-B11, (H27, H28)R2-B31, H16-O15-B11-O17-H18, H34-O33-B31-O35-H36)
17	609	585	174.3161	β_{out}(H9-C4, C6-H10, C12-C2, H14-O13)
18	567	544	423.6407	β_{out}(H16-O15, H18-O17, (H)R1, H34-O33, H36-O35, (H)R2)
19	481	462	205.6319	β_{out}(H16-B11-H18, (H)R1, H34-B31-H36, (H)R2)
20	470	451	84.7	βin(H18-O17-B11-O15-H16, H34-O33-B31-O35-H36)+υ(C2-C12, C22-C30)+β_{in}(C1-C2-C3, C21-C22-C23)

Table 7

Calculated frequencies, scaled frequencies, IR intensity and vibrational assignment of monomer of 4C3FPB

S.N.	Calculated wavenumber (cm^{-1})	Scaled wavenumber (cm^{-1})	IR intensity (a.u.)	Assignment
1	3948	3790	115.9964	υ(O17-H18, O15-H16)
2	3944	3786	20	υ_{as}(O17-H18, O15-H16)
3	3889	3734	109.5757	υ(O13-H14)
4	3385	3250	3.0541	υ_{as}(C3-H8, C4-H9)
5	3382	3247	1.1298	υ_{as}(C1-H7, C6-H10)
6	1941	1864	331.0315	β_{in}(H14-O13-C12-C2)R+υ(O19-C12)
7	1792	1720	3.7638	β_{in}(H8-C3-C4-H9, H7-C1-C6-H10)R+υ(C3-C4, C1-C6)R+υ(C2-C12, C5-B11)
8	1726	1656	17.0806	β_{in}(C12-C2, H8-C3, C4-H9, C1-H7, C6-H10)R+υ_{as}((C2-C3, C6-C5), (C1-C2, C5-C4))R+υ_{as}(C2-C12, C5-B11)
9	1684	1617	15.6049	β_{in}(C12-C2, H8-C3, C4-H9, C1-H7, C6-H10)R+υ_{as}((C2-C3, C6-C5), (C1-C2, C5-C4))R+υ_{as}(C2-C12, C5-B11)
10	1556	1494	123.1663	β_{in}(C12-C2, H8-C3, C4-H9, C1-H7, C6-H10)R+υ_{as}((C3-C4, C1-C6)R+β_{in}(C2-C12, C5-B11)
11	1497	1437	229.3418	β_{in}(O13-H14, C1-H7, C3-H8, C4-H9, C5-B11-O17)+υ(O15-B11)
12	1494	1434	584.1663	β_{in}(H14-O13-C12-O19, C1-H7, C6-H10, B11-O15-H16, B11-O17-H18)+υ(C5-B11)
13	1286	1234	172.4008	β_{in}(H14-O13, C1-H7, C3-H8)+υ(C2-C12)
14	1171	1125	141.6599	υ(O13-C12, C1-C6, C3-C4)+β_{in}(H18-O17, H16-O15, H14-O13)
15	1034	992	169.3322	β_{in}(H18-O17, H16-O15)+υ(B11-O17, B11-O15)
16	956	918	349.3556	β_{in}(H18-O17, H16-O15)
17	816	783	147.4118	β_{out}(H9-C4,C6-H10, C12-C2, H14-O13)
18	704	676	139.0726	β_{out}(H9-C4,C6-H10, C12-C2, H14-O13, C5-B11)
19	614	589	273.7613	β_{out}(C2-C5)R+β_{out}(H14-O13, H18-O17, H16-O15)
20	558	536	102.5634	β_{out}(C2-C5)R+β_{out}(H14-O13, H18-O17, H16-O15)

Abbreviations for modes of vibrations: β_{in} = in plane bending, β_{out} = out of plane bending, ω = wagging, τ = twisting, υ = symmetric stretching, υ_{as} = antisymmetric stretching.

THERMODYNAMIC PROPERTIES

The various thermodynamical parameters at temperature range 100–700 K are computed and listed in Table 8 by using same level theory. The thermodynamic functions are growing with temperature due to the evidence that the molecular vibrational intensities rise with temperature [45]. The correlation graphs are shown in Fig. 7.

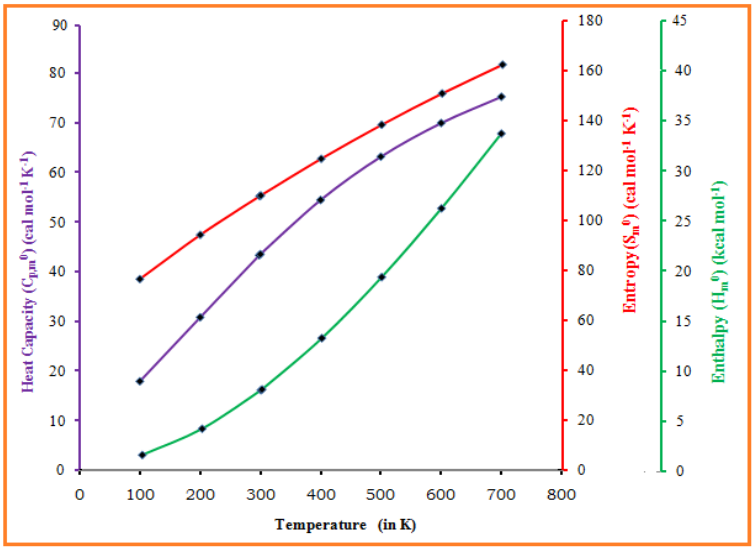

Fig. 7. Correlation charts of heat capacity, entropy, and enthalpy *vs* temperature for 4C3FPB.

The correlation equations between thermodynamic functions specific heat capacity at constant pressure of molecule (C_{pm}), entropy of molecule (S_m), change in enthalpy (ΔH_m), and temperatures were fitted by quadratic formulas and correlation factor are given below.

$$C_{pm} = 1.88526 + 0.16493\ T - 8.55500\times10^{-5}\ T^2\ (R^2 = 0.99972) \quad (8)$$

$$S_m = 58.47438 + 0.18928\ T - 5.88200\times10^{-5}\ T^2\ (R^2 = 0.99996) \quad (9)$$

$$\Delta H_m = -0.73825 + 0.1479\ T - 4.92700\times10^{-5}\ T^2\ (R^2 = 0.99972) \quad (10)$$

Here R^2 gives the value of the correlation constant for each eqation. The entropy, enthalpy and specific heat at particular state m shows good correlation with temperature, however the value of correlation constant for enthalpy and specific heat have the same value, but slightly less than that of entropy. All thermodynamic facts bring supportive statistics for the advance study of 4C3FPB. This statistic may be handy to figure-out some other thermodynamic energy as per relationships of thermodynamic functions and estimate directions of chemical reactions conferring

to second law of thermodynamics in thermo chemical field [51]. It is worth-full to remark here that all thermodynamic calculations were performed in gas phase and they could not be used in solution.

BIOLOGICAL ACTIVITY AND MOLECULAR DOCKING ANALYSIS

Tetko *et al*. [52] develop ALOGPS 2.1 program based on electro topological indices [14, 54, 55] *e.g*. log *P* and log *S*. The predicted value of log *P* (3.21) indicate that title molecule has ability to transport through cell membranes, which establish its pharmacological. The predicted log *S* (–1.93) of title molecule lies in between 85 % drugs which shows that title molecule has better permeability through membranes. The PASS is online server which utilizes several biological activities of title molecule by using SIMILI code of optimized geometry of title molecule. The validity of calculation of various biological activities are based on prediction of a complete more than 8500 drugs which biological activity are experimentally known. The observed biological activities are compared with calculated biological activity predicted by PASS one by one and accuracy of predicted results are 85 % [27]. The molecular mechanisms method utilizes by PASS for prediction of 900 pharmacological effects by using *e.g*. mutagenicity, carcinogenicity, teratogenicity, and embryo toxicity. In Table 8, several biological activities for *P*a > 70 % (*i.e*. *P*a > 0.7) are listed by using PASS online server. From this table, title molecule displays good activities against antineoplastic (0.914), peptidyl transferase inhibitor (0.969), aminoacylase inhibitor (0.960), sugar-phosphatase inhibitor (0.913), ribulose-phosphate 3-epimerase inhibitor (0.896), antiviral (0.862), TP53 expression enhancer (0.860), etc. The TP5 expression enhancer connected with antitumor activity so in this way title molecule have capability to project new antitumor drug. To design new anti-inflammatory in tumor disease this is required to identify the targets, cell which after repressed can kill the affected cells. For this we have performed docking of title molecule to suitable protein by using Swiss-Dock web server [59]. For docking we have uploaded mole2 file of optimized geometry of title molecule and pdb file of selected protein MBNL1 (*Drosophila*) on Swiss dock server [25, 39]. In this process, we have selected all possible conformers of docking with their relative energies value and lowest energy conformers ranked zero. The best binding is ordered according to their full fitness (*FF*) score. To avoid sampling bias docking is performed over whole surface not any specific region of selected protein. The docking figure of title molecule with MBNL1 protein is shown in Fig. 8, by using UCSF chimera. The interaction of title molecule with selected protein are calculated by using binding affinity, *FF* score, and H-bond, bond-length along with amino acids (residue). The hydrogen bond appears in between boron of title molecule residue glycine (GLY-143) with bond length 2.72 Å. The calculated full fitness score –665.44 a.u. with binding affinity (ΔG = –6.56 kcal/mol) suggests good

binding affinity. The docking figure and other calculated parameters shows that title molecule can utilize anti-infantry agent in future.

Table 8

Several biological activities calculated by PASS for *P*a > 0.7

S.N.	Biological activity	*P*a	*P*i
1	Peptidyl transferase inhibitor	0.969	0.000
2	Aminoacylase inhibitor	0.960	0.001
3	Testosterone 17beta-dehydrogenase ($NADP^+$) inhibitor	0.918	0.004
4	Sugar-phosphatase inhibitor	0.913	0.004
5	Cutinase inhibitor	0.899	0.003
6	Glutamyl endopeptidase II inhibitor	0.899	0.003
7	Ribulose-phosphate 3-epimerase inhibitor	0.896	0.003
8	Antiviral	0.862	0.003
9	TP53 expression enhancer	0.860	0.003

Note: *P*a stands for probability 'to be active', and that of *P*i is the probability 'to be inactive'.

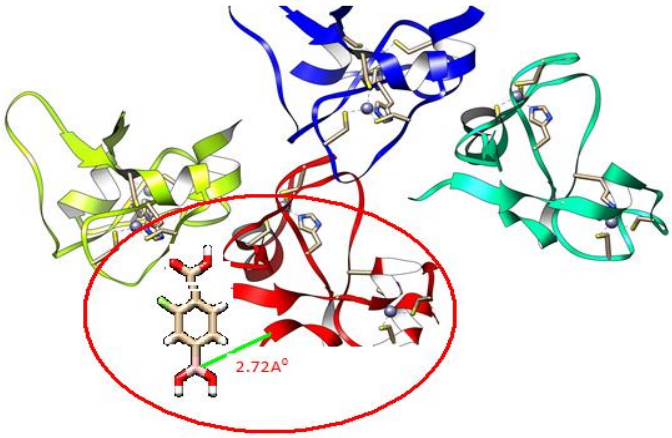

Fig. 8. Molecular docking of title molecule with MBNL1 protein.

CONCLUSIONS

A complete conformational analysis was executed in the forms of 2D and 3D potential energy scans. The cis-trans structure possesses most stable conformer among four stable conformers. Theoretically computed optimized geometric data were matched with the structurally similar compounds in lack of experimental figures. The QTAIM analysis shows that most stable dimer conformer of title molecule exists with two nonbonding interactions. The NBO analysis shows that

charge transfer from n1(O37) $\rightarrow$[σ*(O13–H14)], n3(O19)$\rightarrow$[σ*(H38-O32)] stabilized dimer of title molecule up to 61.88 kcal/mol and 45.66 kcal/mol, respectively. The thermodynamical reaction parameters for dimerization shows that dimerization reaction is exothermic and proceed spontaneous along forward direction. The current communication on 4C3FPB, all together, may communicate the sound interconnection between the geometric structure and NLO response in the shape of hyperpolarizability (β_{total}). Calculations shows the mean polarizability and total first static hyperpolarizability (β_{total}) of the 4C3FPB as 16.3361×10^{-24} e.s.u and 1.1984×10^{-30} e.s.u. respectively. The electronic properties and correlations between statistical thermodynamic factors versus temperature are also established. The large β_{total} value of title compound indicates that this is a bright prospective for NLO material. The docking of MBNL1 with title molecule shows that title molecule has potential for anti-inflammatory agent in future.

Acknowledgement. Author, Anoop Kumar Pandey, is grateful and thanks to the Uttar Pradesh government (India) [No:46/2021/603/sattar-4-2021-4(56)/2020] for providing him with financial support.

REFERENCES

1. ALAM, F., A.H. SOLOWAY, R.F. BARTH, N. MAFUNE, D.M. ADAM, W.H. KNOTH, Boron neutron capture therapy: linkage of a boronated macromolecule to monoclonal antibodies directed against tumor-associated antigens, *J. Med. Chem*., 1989, **32**(10), 2326–2330.
2. ALBERTOA, R., U. ABRAMB, International year of the periodic table 2019: elements important for life sciences, *Chimia*, 2019, **73**(3), 207–209.
3. ANDERSON, M.D., Cancer center. Talabostat and pembrolizumab for the treatment of advanced solid cancers, *ClinicalTrials.gov*. November 20, 2019, Identifier: NCT04171219.
4. ANDRAUD, C., T. BROTIN, C. GARCIA, F. PELLE, P. GOLDNER, B. BIGOT, A. COLLET, Theoretical and experimental investigations of the nonlinear optical properties of vanillin, polyenovanillin, and bisvanillin derivatives, *J. AM. Chem. Soc*., 1994, **116**(5), 2094–2102.
5. BADER, R.F.W., *Atoms in Molecules – A Quantum Theory*, Oxford University Press, Oxford, 1990.
6. BAKER, S.J., C.Z. DING, T. AKAMA, Y.K. ZHANG, V. HERNANDEZ, V. HERNANDEZ, *et al*., Therapeutic potential of boron-containing compounds, *Future Med. Che*., 2009, **1**, 1275–1288.
7. BECKE, A.D., Density-functional thermochemistry. III. The role of exact exchange, *J. Chem. Phys*., 1993, **98**, 5648–5652.
8. CAMBRE, J.N., B.S. SUMERLIN, Biomedical applications of boronic acid polymers, *Polymer*, 2011, **52**, 4631–4643.
9. CHANDRAN, A., H.T. VARGHESE, Y.S. MARY, C.Y. PANICKER, T.K. MANOJKUMAR, C.V. ALSENOY, G. RAJENDRAN, FT-IR, FT-Raman and computational study of (E)-N-carbamimidoyl-4-((4-methoxybenzylidene)amino) benzenesulfonamide, *Spectrochim, Acta. A Mol. Biomol. Spectrosc.*, 2012, **92**, 84–90.
10. CHEN, X., G. LIANG, D., WHITMIRE, J.P., BOWEN, *Ab initio* and molecular mechanics (MM3) calculations on alkyl- and arylboronic acids, *J. Phys. Org. Chem*., 1988, **11**, 378–386.
11. CHONG, P.Y., J.B. SHOTWELL, J.F. MILLER, D.J. PRICE, A. MAYNARD, C. VOITENLEITNER, *et al*., Design of N-benzoxaborole benzofuran GSK8175 – optimization of human pharmacokinetics inspired by metabolites of a failed clinical HCV inhibitor, *J. Med. Chem*., 2019, **62**, 3254–3267.

12. COHEN, H.D., C.C.J. ROOTHAN, Electric dipole polarizability of atoms by the Hartree-Fock Method I: Theory for closed-shell systems, *J. Chem. Phys*., 1965, **43**(10), S34–S38.
13. CUTHBERTSON, E., *Boronic Acids: Properties and Applications*, Alfa Aesar: A Johnson Matthey Company, Heysham, UK, 2006.
14. ESPINOSA, E., I. ALKORTA, J. ELGUERO, E. MOLINS, From weak to strong interactions: A comprehensive analysis of the topological and energetic properties of the electron density distribution involving X–H···F–Y systems, *J. Chem. Phys*., 2002, **117**, 5529–5542.
15. FERNANDES, G.F.S., W.A. DENNY, J.L.D. SANTOS, Boron in drug design: Recent advances in the development of new therapeutic agents, *Eur. J. Med. Chem*., 2019, **179**, 791–804.
16. McDOWELL, L., B. OLIN, Crisaborole: A novel nonsteroidal topical treatment for atopic dermatitis, *J. Pharm. Technol*., 2019, **35**(4), 172–178.
17. FLEMING, I., *Frontier Orbitals and Organic Chemical Reactions*, John Wiley and Sons, New York, 1976.
18. FRANKLAND, E., B.F. DUPPA, Vorläufige Notiz über Boräthyl, *Justus Liebigs Annalen Der Chemie*, 1860, **115**(3), 319–322.
19. FRISCH, E., H.P. HRATCHIAN, R.D. DENNINGTON II, T.A. KEITH, J. MILLAM, B. NIELSEN, A.J. HOLDER, J. HISCOCKS, *Gaussian, Inc., GaussView Version 5.0.8*, 2009.
20. FRISCH, M.J., G.W. TRUCKS, H.B. SCHLEGEL, *et al*., *Gaussian Inc., Wallingford, CT*, 2009.
21. GESKIN, V.M., C. LAMBERT, J.L. BREDAS, Origin of high second- and third-order nonlinear optical response in ammonio/borato diphenylpolyene zwitterions: the remarkable role of polarized aromatic groups, *J. Am. Chem. Soc*., 2003, **125**(50), 15651–15658.
22. GROLL, M., C.R. BERKERS, H.L. PLOEGH, H. OVAA, Crystal structure of the boronic acid-based proteasome inhibitor bortezomib in complex with the yeast 20S proteasome, *Structure*, 2006, **14**, 451–456.
23. HALL, D.G. (Ed.), *Boronic Acids*: *Preparation and Application in Organic Synthesis and Medicine* 1st ed., Wiley-VCH, Weinheim, Germany, 2005, DOI:10.1002/3527606548.
24. HALL, D.G., (Ed), *Boronic Acids*: *Preparation and Applications in Organic Synthesis and Medicine*, Wiley-VCH; Weinheim, Germany, 2011, pp. 1–99.
25. ISHIKAWA, K., T. NAGASE, D. NAKAJIMA, N. SEKI, M. OHIRA, N. MIYAJIMA, A. TANAKA, H. KOTANI, N. NOMURA, O. OHARA, Prediction of the coding sequences of unidentified human genes. VIII. 78 New cDNA clones from brain which code for large proteins *in vitro*, *DNA Research*, 1997, **4**(5), 307–313.
26. JORGENSEN, W.L., E.M. DUFFY, Prediction of drug solubility from Monte Carlo simulations, *Bio. Org. Med. Chem. Lett*., 2000, **10**(11), 1155–1158.
27. KAHLERT, J., C.J.D. AUSTIN, M. KASSIOU, L.M. RENDINA, The fifth element in drug design: Boron in medicinal chemistry, *Chem. Inform*., 2013, **66**, 1118–1123.
28. KLEINMAN, D.A., Nonlinear dielectric polarization in optical media, *Phys. Rev*.,1962, **126**, 1977–1979.
29. KOCH, U., P. POPELIER, Characterization of C–H–O hydrogen bonds on the basis of the charge density, *J. Phys. Chem*., 1995, **99**(24), 9747–9754.
30. KOHN, W., L.J. SHAM, Self-consistent equations including exchange and correlation effects, *Phys. Rev*., 1965, **140**, A1133–A1138.
31. KRISHNAKUMAR, V., R. RAMASAMY, DFT studies and vibrational spectra of isoquinoline and 8-hydroxyquinoline, *Spectrochim. Acta A*, 2005, **61**, 673–683.
32. KRISHNAKUMAR, V., R.J. XAVIER, T. CHITHAMBARATHANU, Density functional theory study of the FT-IR spectra of phthalimide and N-bromophthalimide, *Spectrochim. Acta A*, 2005, **62**, 918–925.
33. KUMAR, S.K., E. HAGER, C. PETTIT, H. GURULINGAPPA, N.E. DAVIDSON, S.R. KHAN, Design, synthesis, and evaluation of novel boronic-chalcone derivatives as antitumor agents, *J. Med. Chem*., 2003, **46**, 2813–2815.

34. LEE, C., W. YANG, R.G. PARR, Development of the Colle-Salvetti correlation-energy formula into a functional of the electron density, *Phys. Rev. B.*,1998, **37**, 785–789.
35. LIU, B., R.E.L. TROUT, G.H. CHU, D. MCGARRY, R.W. JACKSON, J.C. HAMRICK, D.M. DAIGLE, S.M. CUSICK, C. POZZI, F.D. LUCA, M. BENVENUTI, S. MANGANI, J.D. DOCQUIER, W.J. WEISS, D.C. PEVEAR, L. XERRI, C.J. BURNS, Discovery of taniborbactam (VNRX-5133): A broad-spectrum serine- and metallo-b-lactamase inhibitor for carbapenem-resistant bacterial infections, *J. Med. Chem*., 2020, **63**, 2789–2801.
36. MCNAUGHT, A.D., A. WILKINSON, *IUPAC. Compendium of Chemical Terminology. The ''Gold Book''*, second ed., Blackwell Scientific Publications, Oxford, 1997.
37. MERRICK, J.P., D. MORAN, L. RADOM, An evaluation of harmonic vibrational frequency scale factors, *J. Phys. Chem. A*, 2007, **111**, 11683–11700.
38. MIEHLICH, B., A. SAVIN, H. STOLL, H. PREUSS, Results obtained with the correlation energy density functionals of Becke and Lee, Yang and Parr, *Chem. Phys. Lett*. 1989, **157**(3), 200–206.
39. MILLER, J.W., C.R. URBINATI, P. TENG-UMNUAY, M.G. STENBERG, B.J. BYRNE, C.A. THORNTON, M.S. SWANSON, Recruitment of human muscleblind proteins to (CUG)(n) expansions associated with myotonic dystrophy, *The EMBO Journal*, 2000, **19**, 4439–4448.
40. OBOYLE, N.M., A.L. TENDERHOLT, K.M. LANGNER, Cclib: a library for package independent computational chemistry algorithms, *J. Comp. Chem*., 2008, **29**, 839–845.
41. OTT, J.B., J. BOERIO-GOATES, *Calculations from Statistical Thermodynamics*, Academic Press, Cambridge, 2000.
42. PEARSON, R.G., The principle of maximum hardness, *Acc. Chem. Res*., 1993, **26**, 250–255.
43. PETASIS, N.A., Expanding roles for organoboron compounds versatile and valuable molecules for synthetic, biological and medicinal chemistry, *Aust. J. Chem*., 2007, **60**, 795–798.
44. PIPEK, J., P.Z. MEZEY, A fast intrinsic localization procedure applicable for ab initio and semiempirical linear combination of atomic orbital wave functions, *J. Chem. Phys*., 1989, **90**, 4916–4926.
45. RETTIG, S.J., J. TROTTER, Crystal and molecular structure of phenylboronic acid, C6H5B(OH), *Can. J. Chem*., 1977, **55**, 3071–3075.
46. RICHARDSON, P.G., T. HIDESHIMA, K.C. ANDERSON, Bortezomib (PS-341): A novel, first-in-class proteasome inhibitor for the treatment of multiple myeloma and other cancers, *Canc. Contr*., 2003, **10**, 361–369.
47. ROZAS, I., I. ALKORTA, J. ELGUERO, Behavior of ylides containing N, O, and C atoms as hydrogen bond acceptors, *J. AM. Chem. Soc*., 2000, **122**(45), 11154–11161.
48. SAJAN, D., L. JOSEPH, N. VIJAYAN, M. KARABACAK, Natural bond orbital analysis, electronic structure, non-linear properties and vibrational spectral analysis of L-histidinium bromide monohydrate: A density functional theory, *Spectrochim. Acta A*, 2011, **81**(1), 85–98.
49. SMITH, T.P., I.W. WINDSOR, K.T. FOREST, R.T. RAINES, Stilbene boronic acids form a covalent bond with human transthyretin and inhibit its aggregation, *J. Med. Chem*., 2017, **60**, 7820–7834.
50. SUN, Y.X., Q.L. HAO, W.X. WEI, Z.X. YU, L.D. LU, X. WANG, Y.S. WANG, Experimental and density functional studies on 4-(3,4-dihydroxybenzylideneamino) antipyrine, and 4-(2,3,4-trihydroxybenzylidene-amino) antipyrine, *J. Mol. Struct.: Theochem*., 2009, **904**, 74–82.
51. TETKO, I. V. Neural network studies. 4. Introduction to associative neural networks, *J. Chem. Inf. Comput. Sci*., 2002, **42**(3), 717–728.
52. TETKO, I.V., V.Y. TANCHUK, T.N. KASHEVA, A.E. VILLA, Estimation of aqueous solubility of chemical compounds using E-state indices, *J. Chem. Inf. Comput. Sci*., 2001, **41**(6), 1488–1493.
53. TJARKS, W., A.K.M. ANISUZZAMAN, L. LIU, S.H. SOLOWAY, R.F. BARTH, D.J. PERKINS, D.M. ADAMS, Synthesis and in vitro evaluation of boronated uridine and glucose derivatives for boron neutron capture therapy, *J. Med. Chem*., 1992, **35**(9), 1628–1633.

54. TRIPPIER, P.C., C. MCGUIGAN, Boronic acids in medicinal chemistry: anticancer, antibacterial and antiviral applications, *Med. Chem. Commun*., 2010, **1**(3), 183–198.
55. WINDSOR, I.W., M.J. PALTE, J.C. LUKESH, B. GOLD, K.T. FOREST, R.T. RAINES, Sub-picomolar inhibition of HIV-1 protease with a boronic acid, *J. Am. Chem. Soc*., 2018, **140**, 140–158.
56. WU, Y. M., C.C. DONG, S. LIU, H.J. ZHU, Y.Z. WU, 3-Fluorophenylboronic acid, *Acta Cryst. E*, 2006, **62**, 4236–4237.
57. YAMAMOTO, Y., Molecular design and synthesis of B-10 carriers for neutron capture therapy, *Pure Appl. Chem*., 1991, **63**, 423–426.
58. YANG, W., X. GAO, B. WANG, Boronic acid compounds as potential pharmaceutical agents. *Med. Res. Rev*., 2003, **23**, 346–368.
59. ***www.swissdock.ch.